scientific reports

Check for updates

OPEN

hsa-mir-483-3p modulates delayed breast cancer recurrence

Ok-Hyeon Kim[1,5], Tae Jin Jeon[2,5], Hana Kang[2], Eun Seo Chang[2], Soon Auck Hong[3], Min Kyoon Kim[4]✉ & Hyun Jung Lee[1,2]✉

Patients with estrogen receptor-positive breast cancer undergoing continuous adjuvant hormone therapy often experience delayed recurrence with tamoxifen use, potentially causing adverse effects. However, the lack of biomarkers hampers patient selection for extended endocrine therapy. This study aimed to elucidate the molecular mechanisms underlying delayed recurrence and identify biomarkers. When miRNA expression was assessed in luminal breast cancer tissues with and without delayed recurrence using NanoString, a significant increase in the expression of miR483-3p was observed in samples from patients with delayed recurrence compared with those without. miR483-3p expression was elevated in tamoxifen resistant (TAMR) EFM19 cells than in non-resistant EFM19 cells. Notably, genes associated with cancer metastasis (*AMOTL2*, *ANKRD1*, *CTGF*, and *VEGF*) were upregulated in TAMR EFM19 cells, although cell motility and proliferation were reduced. Transfection of miR483-3p mimics into both non-resistant EFM19 and MCF7 cells resulted in increased expression of cancer metastasis-related genes, but decreased proliferation and migration. Given that miR483-3p can bind to the 3′UTR region of O-GlcNAc transferase (*OGT*) and potentially affect its protein expression, we examined OGT protein levels and found that transfection with miR483-3p mimics selectively reduced OGT expression. Overall, breast cancer cells subjected to long-term hormone therapy displayed elevated miR483-3p expression, reducing motility and dormancy induction via decreased OGT expression. These findings suggest that miR483-3p is a potential biomarker for long-term endocrine therapy.

Keywords Breast cancer, Delayed recurrence, miR483-3p, Dormancy

Abbreviations

TAMR	Tamoxifen-resistant
OGT	O-GlcNAc transferase
ERN	Estrogen receptor negative
ERP	Estrogen receptor positive
AMOTL2	Angiomotin-like protein 2
ANRKD1	Ankyrin repeated domain 1
CTGF	Connective tissue growth factor
VEGF	Vascular endothelial growth factor
AGO2	Argonaute 2
TARBP2	Trans-activation-responsive RNA-binding protein 2
PR	Progesterone receptor
HER2	Human epidermal growth factor receptor 2
PLOD2	Procollagen-lysine, 2-oxoglutarate 5-dioxygenase 2
KRT80	Keratin 80
eIF4E	Eukaryotic initiation factor 4E
HCC	Hepatocellular carcinoma
CDKN1A	Cyclin dependent kinase inhibitor 1 A
CDK	Cyclin dependent kinase
EMT	Epithelial-mesenchymal transition
O-GlcNAc	O-linked β-D-N-acetylglucosamine

[1]Department of Anatomy and Cell Biology, College of Medicine, Chung-Ang University, Seoul 06974, South Korea. [2]Department of Global Innovative Drugs, Graduate School of Chung-Ang University, Seoul 06974, South Korea. [3]Department of Pathology, College of Medicine, Chung-Ang University, Seoul 06974, South Korea. [4]Department of Surgery, College of Medicine, Chung-Ang University, Seoul 06974, South Korea. [5]Ok-Hyeon Kim and Tae Jin Jeon contributed equally to this work. ✉email: mkkim96@cauhs.or.kr; pluto38@cau.ac.kr

O-GlcNAcylation O-linked β-N-acetylglucosamine modification

After the initial treatment for breast cancer, a unique nonlinear temporal pattern associated with the subsequent risk of recurrence and death occurs. Notably, variations in the recurrence patterns of breast cancer over time appear to differ based on breast cancer subtype. The overall risk of early recurrence is much higher in patients with Estrogen Receptor (ER)-negative (N) tumors; however, the second peak of recurrence is attributed to ER-positive (P) tumors[1]. The delayed recurrence pattern observed in hormone-responsive breast cancer is a unique characteristic that distinguishes it from other typical cancers. While the survival rates for patients with breast cancer are generally higher than those for patients with other cancer types, those with ERP continue to harbor concerns about recurrence, even up to 10 or 20 years after the initial diagnosis. Therefore, in the treatment of ERP breast cancer, emphasis is placed not only on short-term adjuvant chemotherapy but also on long-term adjuvant endocrine therapy, recognizing its critical importance.

Administering adjuvant endocrine therapy for an extended period of 10 years, rather than the conventional 5 years, produces a reduction in the hazard ratio of approximately 0.7 for both breast cancer recurrence and breast cancer-specific mortality after the first decade[2,3]. Current guidelines recommend ten years of adjuvant endocrine therapy for patients with ERP, unless there are characteristics of an extremely low-risk disease[4,5]. However, definite long-term side effects of tamoxifen, such as endometrial cancer and thromboembolic events, are observed[6]. Currently, the main challenge for clinicians is appropriate selection of patients who can receive extended endocrine therapy. Understanding the mechanisms underlying the delayed recurrence of hormone-responsive breast cancer may assist in identifying patients who may benefit from the extension of hormone therapy or those who may require additional treatment, such as CDK 4/6 inhibitors. However, the best biomarker for determining the optimal patients at risk of delayed recurrence has not yet been developed.

The recent emergence of miRNAs, small non-protein-coding RNA that play important roles in tumor initiation and progression, has presented new opportunities for cancer diagnosis[7,8]. MiRNAs are regulatory non-coding RNA molecules that are 16–25 nucleotides in length. These molecules regulate gene expression through posttranslational mechanisms, including mRNA degradation and translation repression. Accumulating evidence has shown that miRNA expression is dysregulated in human malignancies. In particular, abnormal miRNA expression in malignant cells compared to normal cells is often attributed to alterations in genomic miRNA copy numbers and gene locations (amplification, deletion, or translocation). In lung cancer, the 5q33 region harboring miR-143 and miR-145 is often deleted, resulting in the decreased expression of both miRNAs[9]. In addition, miRNA expression can be tightly controlled by different transcription factors; therefore, abnormal expression of miRNAs in cancer may be attributed to the dysregulation of key transcription factors, such as c-Myc[10,11]. Moreover, the identification of tumor-specific alterations in the miRNA processing machinery, such as in genes encoding *TARBP2*, *AGO2*, *Dicer*, and Exportin-5 (*XPO5*), provides strong evidence that these pathways are relevant to cellular transformation[12]. Thus, miRNA expression signatures and their profiles can be used as biomarkers to predict the prognosis of diseases or diagnose cancers[13,14].

In the present study, we investigated the expression profiles of miRNAs in samples from patients with delayed recurrence. We aimed to elucidate the molecular mechanisms through which the identified miRNAs are associated with late recurrence.

Methods

Ethical considerations

The research was performed according to the Declaration of Helsinki including patients' consent. The study was approved by the Institutional Review Board of the Chung-Ang University Hospital.

Patient samples and miRNA screening

miRNA expression was analyzed in luminal breast cancer tissues that exhibited delayed recurrence after 5 years of primary treatment and in those that showed no recurrence using the NanoString technique.

From 2008 to 2012, we selected consecutive six patients diagnosed with stage I-III ER-positive, HER2-negative breast cancer who experienced delayed recurrence at the Chung-Ang University Hospital through a review of medical records. For comparison, we selected six additional control patients with similar clinical characteristics, including diagnosis timing, stage, and age, but without recurrence. The detailed information of patients' clinicopathologic characteristics, treatment, and recurrence are described in Supplementary Table. Formalin-fixed paraffin-embedded (FFPE) tissues were prepared from surgical specimens obtained during the initial treatment of each patient. This study was approved by the Institutional Research Integrity Board of the Chung-Ang University Hospital (IRB number: 2301-019-539). Nucleic acids were retrieved from FFPE RMS tumor tissue scrolls, and total RNA was extracted using the Qiagen RNeasy FFPE kit (Qiagen, 73504, USA).

RNA with a 260/230 nm absorbance ratio > 1.8 and 260/280 nm absorbance ratio > 1.8 was used for subsequent experiments on the NanoString nCounter platform[15]. After completion of the hybridization reaction, RNA samples were transferred to the Prep station. The Prep station removes samples where capture and report probes do not bind simultaneously, fixing only those samples where both types of probes accurately bind to RNA on the cartridge. The prepared cartridge was then transferred to a Digital Analyzer (NanoString, nCounter Digital Analyzer, NCT-DIGT-120, USA). The fluorescent barcodes attached to each probe were counted using an internal microscope in a Digital Analyzer, and the expression of each gene was read using probe sets. The Reporter Code Count (RCC) file obtained by counting in the Digital Analyzer underwent quality control, leading to the measurement of normalization and fold-change values. For each sample, a significant change was considered when comparing the fold change with that of the control group, showing either an increase of at least 2-fold or decrease of at least 2-fold.

Cell culture

Human breast cancer cell lines, EFM19, MDA-MB-415 and MCF7, were purchased from the American Type Culture Collection (ATCC, USA) and cultured according to the accompanying guidelines. EFM19 and MCF7 cells were cultured in Roswell Park Memorial Institute medium (RPMI) 1640 (Welgene, Korea), and MDA-MB-415 cells were maintained in Dulbecco's Modified Essential Medium (EMEM, Welgene, Korea) supplemented with 10% fetal bovine serum (FBS; AbFrontier, Korea) and 1% penicillin and streptomycin antibiotics (Gibco, USA). The cells were maintained in a humidified incubator at 37 °C with 5% CO_2. Tamoxifen-resistant EFM19 cells have been established for at least one year[16]. Briefly, 5×10^5 cells per well were plated in 6-well plates (SPL, Korea) and cultured for 24 h. After 24 h, cells were replaced with 5% FBS/RPMI1640 or DMEM medium containing 1 μM 4-OH tamoxifen (Sigma, H6278-10MG). Finally, the concentration of 4-OH tamoxifen was gradually increased up to 5 μM. The tamoxifen-supplemented medium was changed every 2 days.

Cell viability assay

Cell viability was assessed using an alamarBlue assay kit (Invitrogen, USA) following the manufacturer's instructions. Cells were seeded at a density of 1,000 cells per well in 96-well culture plates (Thermo Fisher Scientific) and allowed to adhere overnight. The medium was replaced with fresh medium and cell viability was measured at 12 h intervals for up to 48 h. At the end of the experiment, 10% (v/v) alamarBlue solution was added to each well. After incubation for 1 h, the fluorescence intensity was detected using a Synergy LX Multi-Mode Reader (Agilent Technologies, USA) at excitation wavelengths of 530 and 590 nm. All assays were performed in triplicate.

Time-lapse imaging

To quantify cell motility, a 6-well plate was placed under an inverted microscope (Eclipse Ti2, Nikon, Japan). Images were recorded every 3 min for 6 h in an environmental chamber maintained at 37 °C in 5% CO_2. Cellular motility was observed by time-lapse image sequencing using the manual tracking plug-in for ImageJ (http://rsb.info.nih.gov/ij) software. ImageJ output was integrated into the Chemotaxis and Migration Tool software (ibidi GmbH, Germany) to determine the migration position and velocity of the cells in each well.

Wound healing assay

Cells were seeded in 6-well plates and allowed to grow to form a confluent monolayer. At approximately 100% confluency, cells were scraped using a 200 μL micropipette tip. Immediately after scraping, the medium was replaced with a fresh medium. Images of the wound area were monitored under a phase-contrast microscope (Olympus IX-81, Japan) for 48 h. The wound gap was measured using ImageJ software, and wound closure was calculated according to the following formula:

$$\text{Wound closure } (\%) = \frac{\text{Width of the wound}_{0\text{ h}} - \text{Width of the wound}_{24\text{ h}}}{\text{Width of the wound}_{0\text{ h}}} \times 100$$

RNA expression and quantitative RT-PCR

Total RNA was extracted using the RNeasy Mini Kit (Qiagen, Germany) according to the manufacturer's instructions. RNA was reverse transcribed using a Maxima First Strand cDNA Synthesis Kit (Thermo Fisher Scientific, USA). The synthesized cDNA and 2× SYBR Green PCR Master Mix (Applied Biosystems, USA) were used in 20 μL reactions. Cycle thresholds (Ct) were determined using the StepOnePlus Real Time PCR System (Applied Biosystems, USA) and mRNA expression was normalized to *GAPDH* and the control sample. To analyze miRNA expression, miRNAs were isolated using a mirVANA miRNA isolation kit (Thermo Fisher Scientific) according to the manufacturer's instructions. cDNA was synthesized from total RNA using TaqMan miRNA primers for miR-483-3p, miR483-3p-mimic (Applied Biosystems), and the TaqMan MicroRNA Reverse Transcription kit (Applied Biosystems). cDNA was synthesized using the TaqMan Fast Advanced Master Mix (Thermo Fisher Scientific). qRT-PCR was performed using a StepOnePlus Real Time PCR System (Applied Biosystems), and the RNU48 transcript was used as a normalizing control.

Transfection of miRNA

miRNA transfection was performed using DharmaFECT 1 (Dharmacon, USA), according to the manufacturer's instructions. Cells were plated at 3×10^5 cells in a 6-well plate and transfected with miR-483-3p mimics or control miR (Bioneer, Korea). After incubation for 24 h, the transfection efficiency was confirmed using qRT-PCR.

Immunoblotting

Cells were harvested in a RIPA lysis and extraction buffer (Thermo Fisher Scientific) containing 1% protease and phosphatase inhibitor cocktails (Sigma-Aldrich, USA). Equal amounts of proteins were separated using sodium dodecyl sulfate-polyacrylamide gel electrophoresis (SDS-PAGE) and analyzed by immunoblotting. Immunoblotting was performed following standard procedures using anti-YAP (1:1000, Cell Signaling Technology, Danvers, MA, USA), anti-TAZ (1:1000, BD Biosciences), anti-PD-L1 (1:1000, Cell Signaling Technology), anti-OGT (1:1000, Cell Signaling Technology), and anti-GAPDH (G-9) (1:1000, SantaCruz Biotechnology, sc-365062, USA) antibodies. Gel images were captured using the ImageQuant LAS4000 system (GE Healthcare Life Sciences, USA).

Statistical analysis

Statistical analyses were performed using GraphPad Prism Version 9 (GraphPad, Inc., USA). All data were analyzed as the mean ± standard error of the mean (SEM), and *p*-values were determined using an unpaired

t-test and one-way analysis of variance (ANOVA). Significant differences between the groups were established using the following *p*-values: $^{*}p < 0.05$, $^{**}p < 0.01$, $^{***}p < 0.001$, and $^{****}p < 0.0001$.

Results

MiR-483-3p expression was correlated with delayed recurrence and survival probability

Gene expression changes were examined using fold changes in breast cancer tissues that showed delayed recurrence compared to those without recurrence. In tissues with delayed recurrence, miR-483-3p and miR-1260b were significantly upregulated, whereas miR-450a-5p, miR-495-3p, miR-31-5p, miR-503-5p, miR-223-3p, and miR-424-5p were downregulated (Fig. 1A). Among them, miR-483-3p, which is strongly associated with the onset of breast cancer through its involvement in the M phase of the cell cycle, cell cycle regulation, programmed cell death, and cell proliferation, was deemed to be a significant factor. In addition, staining for miR-483-3p in 137 tumor microarrays showed high expression in 15 cases and low expression in 122 cases and the expression level of miR-483-3p was closely correlated with survival probability (Fig. 1B). Therefore, subsequent experiments focusing on miR-483-3p were conducted.

Oncoprotein expression is increased in tamoxifen resistant breast cancer cells

Tamoxifen-resistant (TAMR) cell lines were developed to simulate the delayed recurrence of breast cancer induced by long-term hormone therapy. Briefly, human breast cancer cell line with ER + PR + HER2- luminal A subtype, EFM19 was cultured with 1 μM tamoxifen, with the concentration gradually increased up to 5 μM over a period of 12 months. Once the tamoxifen-resistant cell line was established, the expression of miR483-3p was significantly elevated in TAMR EFM19 cells than in parental EFM19 cells (Fig. 2A). When establishing a tamoxifen-resistant cell line using the MDA-MB-415 breast cancer cell line (ER + PR + HER2-, luminal A subtype), miR-483-3p expression similarly increased in TAMR MDA-MB-415 cells compared to parental MDA-MB-415 (Supplementary Fig. 1).

Recent studies suggest that the YAP pathway may be linked to hormone therapy resistance in breast cancer[17–19]. Therefore, YAP/TAZ and their downstream target genes were evaluated in TAMR EFM19 cells. Interestingly, the protein expression of YAP and TAZ, as well as the gene expression of downstream targets *ANKRD1*, *AMOTL2*, and *CTGF* were elevated in TAMR EFM19 compared to parental EFM19 cells (Fig. 2B and C). In particular, *VEGF*, which is involved in the remodeling of the tumor microenvironment, was also elevated in TAMR EFM19.

Persistent treatment of tamoxifen induces dormant breast cancer cells

The migratory ability or motility of cancer cells is central to the morphogenesis and multiple aspects of tumor metastasis. Parental EFM19 and TAMR EFM19 cells were observed under a live imaging microscope, and their motility was analyzed by manual tracking using ImageJ. The migration speed of TAMR EFM19 cells was significantly lower than that of parental EFM19 cells (Fig. 3A and B). Similarly, parental EFM19 significantly decreased intercellular spacing for up to 48 h, whereas TAMR EFM19 exhibited reduced wound closure (Fig. 3C and D). Overall, these results indicate that cellular motility was largely reduced in TAMR EFM19 cells, suggesting that persistent hormone treatment might induce cancer dormancy in this system[20,21]. Since the most frequently used anticancer therapies target highly proliferative cancer cells, non- or slowly-proliferating dormant cancer cells can persist after treatment, eventually causing tumor relapse[22]. Thus, the expression of dormancy-related genes, *p53* and *p21*, was evaluated to determine whether persistent hormone therapy and its resistance can induce dormancy-like signaling[23]. We found that *p21* and *p53* expression were significantly increased in TAMR EFM19 than in parental EFM19 (Fig. 3E and F).

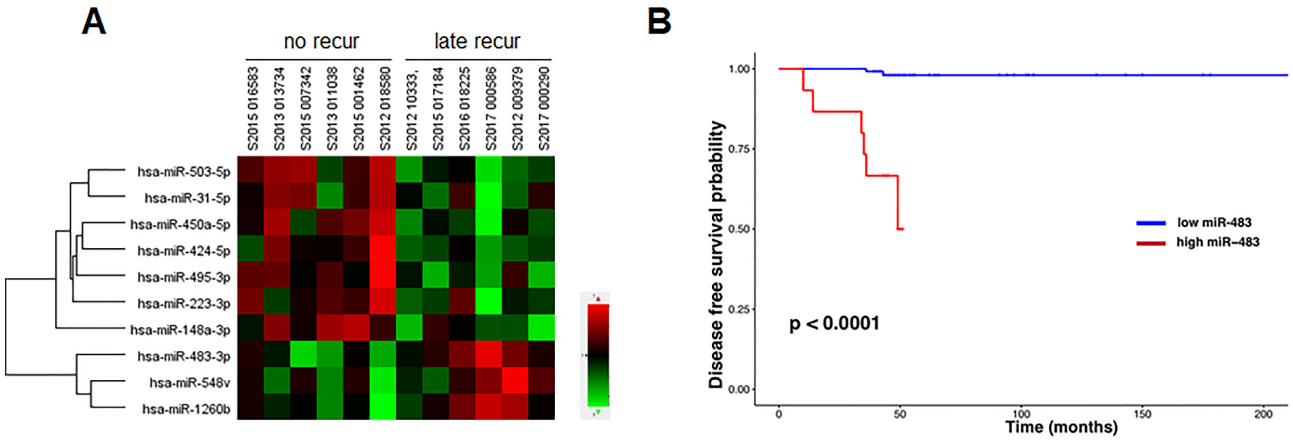

Fig. 1. miRNA screening from patient samples with delayed recurrence or those without. (**A**) Heat map showing the NanoString gene expression profiles of patient samples with delayed recurrence or those without. (**B**) Kaplan–Meier survival curve for miR483-3p associated with overall survival in breast cancer. The x-axis represents overall survival time (months) and the y-axis represents survival function.

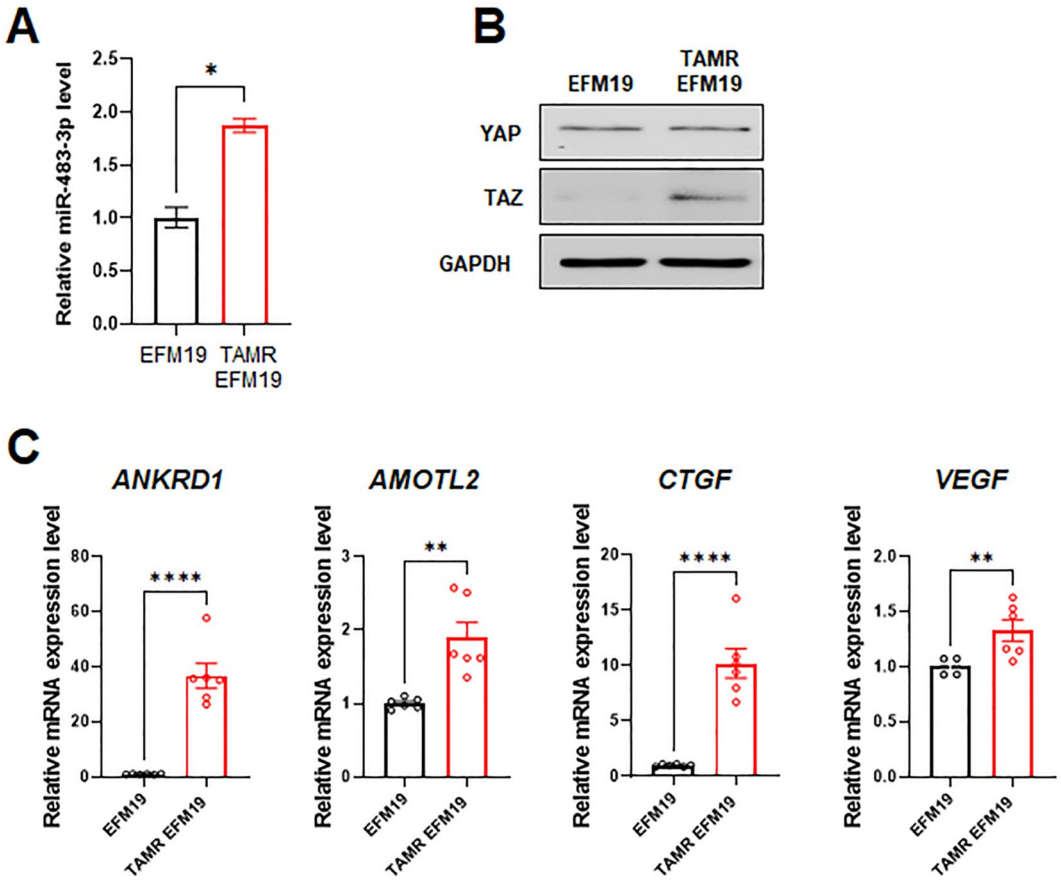

Fig. 2. miR-483-3p and YAP/TAZ signaling appeared enhanced in TAMR breast cancer cell. (**A**) Quantitative RT-PCR results showing the relative indicated miRNA levels in parental EFM19 and TAMR EFM19 cells (unpaired *t*-test, $^{**}p < 0.01$; $n = 3$). (**B**) YAP and TAZ protein levels in parental EFM19 and TAMR EFM19 cells were evaluated using immunoblotting. (C) Quantitative RT-PCR results indicating relative mRNA levels in parental EFM19 and TAMR EFM19 cells (unpaired *t*-test, $^{**}p < 0.01$, $^{****}p < 0.0001$; $n = 3$).

MiR483-3p recapitulates the features of TAMR breast cancer cells

To determine whether the features exhibited by TAMR breast cancer cells, such as slowed motility or enhanced dormancy-related gene expression, were induced by miR483-3p, we transfected parental EFM19 or MCF7 cells with miR483-3p. Notably, when miR483-3p was transfected into each cell line, the cell proliferation rate was significantly reduced in MCF7 and EFM19 cells with miR483-3p than in control cells (Fig. 4A, B, and C). Furthermore, EFM19 cells with miR483-3p exhibited increased tamoxifen resistance compared to EFM19 cells with control miRNA when treated with varying concentrations of tamoxifen (Supplementary Fig. 2). Although cancer progression-related genes, including *AMOTL2*, *ANKRD1*, *CTGF*, *PLOD2* and *KRT80*, were highly elevated in EFM19 cells with miR483-3p (Fig. 4D), their motility was drastically inhibited (Fig. 4E and F), which is consistent with the results observed in TAMR breast cancer cells.

MiR483-3p reduces the expression of O-GlcNAc transferase

To elucidate the molecular mechanisms underlying the involvement of miR483-3p in signaling associated with breast cancer dormancy, we investigated molecules that may be targets of miR483-3p. The software TargetScan predicted the 3′UTR of several genes targeted by miR483-3p. We restricted the high-ranked targets to those reported to be highly expressed in breast cancer or strongly implicated in breast cancer proliferation. As it has been reported that O-linked β-d-N-acetylglucosamine (GlcNAc) transferase (OGT) is highly expressed in several cancers and OGT expression is required for oncogenesis of breast cancer[24,25], we evaluated OGT levels to determine if the OGT 3′UTR is affected by miR483-3p (Fig. 5A, B and C). Notably, OGT protein expression was significantly reduced by both MCF7 and EFM19 cells with miR483-3p, suggesting that continuous tamoxifen-induced miR483-3p interrupts OGT protein expression in breast cancer cells, which may mitigate cancer dormancy.

Discussion

Persistent endocrine therapy in breast cancer induces dormancy and delays recurrence. In this study, we observed elevated miR-483-3p expression in patients experiencing delayed recurrence and consistent increases in miR-483-3p levels in a TAMR cell model mimicking this condition. Notably, ectopic expression of miR-483-

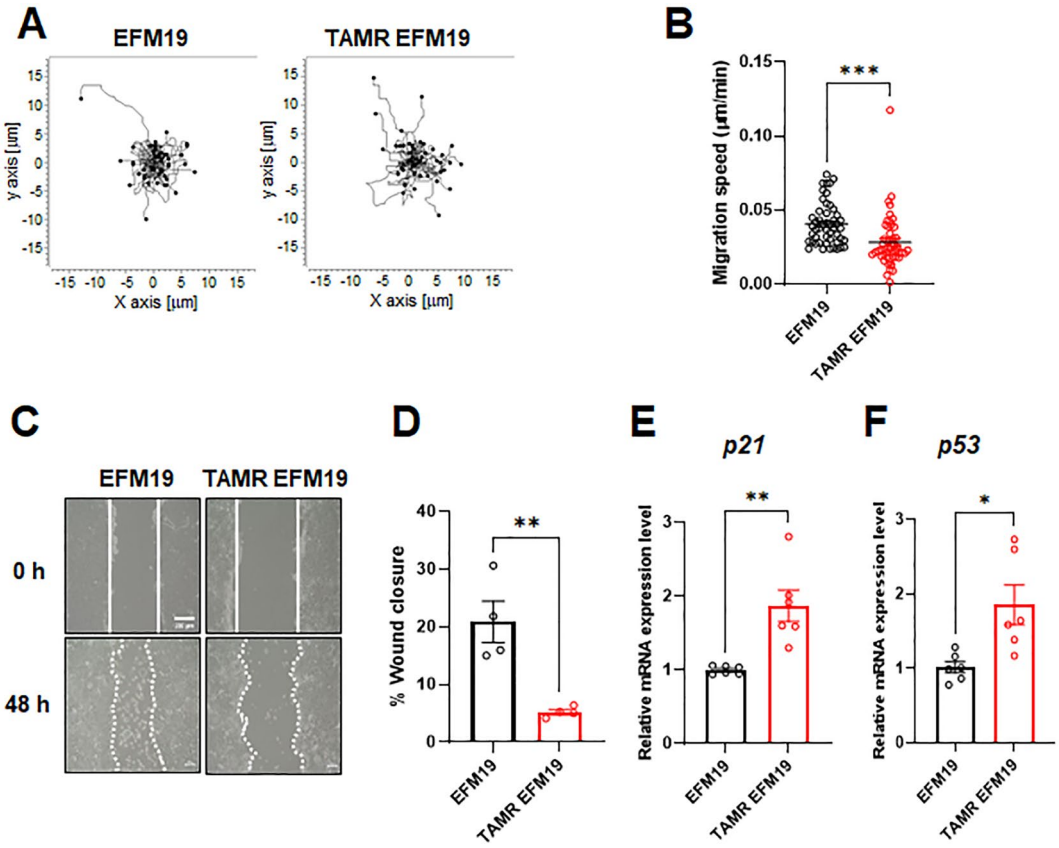

Fig. 3. TAMR EFM19 cells show reduced motility and dormancy in related gene expression. (**A**) Spatial tracking of parental or TAMR EFM19 cell movement during the 6 h time-lapse imaging where each cell lies at the origin (0,0) at t = 0 h. The plots show the motility of individual cells in one representative experiment. Cells are indicated as black dots. The movement of each cell was traced using ImageJ software with a manual tracking plugin. The migration speed graphs were summarized using $n = 50$ individual cell tracking results. (**B**) Quantification of migration speed revealed the cellular velocities of individual cells ($n = 3$ independent experiments; unpaired t-test, $^{***}p < 0.001$). (**C**) Wound healing ability in parental EFM19 and TAMR EFM19 cells. Photos were captured at 0 h and 48 h. The closed area indicated by the white line was quantified using ImageJ software. Scale bar = 200 µm. (**D**) Graph shows the percentage wound closure as quantified using ImageJ software ($n = 4$; unpaired t-test, $^{**}p < 0.01$). (**E,F**) Gene expression levels of *p53* and *p21* in parental and TAMR EFM19 cells were evaluated by quantitative real-time reverse transcription polymerase chain reaction experiments (qRT-PCR; $n = 3$ independent experiment, unpaired t-test, $^{*}p < 0.05$, $^{**}p < 0.01$).

3p in parental breast cancer cell lines induces characteristics associated with delayed recurrence, such as reduced cell proliferation and migration.

Notably, miR-483-3p binds to the 3′UTR of OGT, reducing its protein expression. O-GlcNAcylation, mediated by OGT, modifies protein–protein interactions, protein stability, and phosphorylation states. Both OGT and O-GlcNAcylation are upregulated in various cancers and drive tumor growth, metastasis, and drug resistance[26,27]. For instance, OGT modifies eukaryotic initiation factor 4E (eIF4E), a key regulator of translation, in liver cancer, and its high expression correlates with a poor prognosis in hepatocellular carcinoma (HCC)[28]. Furthermore, OGT enhances the stem cell potential of HCC cells by upregulating eIF4E. Similarly, increased OGT expression in breast cancer cells boosts tumor initiation capacity and stem cell marker expression[24,29]. These findings suggest that miR-483-3p inhibition of OGT may attenuate breast cancer cell proliferation and migration, thereby inducing a quiescent state.

In this study, we demonstrated that YAP/TAZ and their downstream target genes are elevated in TAMR cells, consistent with previous findings[17–19]. Notably, the YAP pathway appears to regulate ERα expression at the transcriptional level by directly binding to regulatory regions of the ERα-encoding gene. Forced activation of the YAP pathway reduces ERα expression, contributing to tamoxifen resistance in breast cancer. Although the relationship between the YAP pathway and miR-483-3p was not assessed in this study, further investigation into this potential interaction may provide valuable insights.

Our research demonstrated elevated *p53* and *p21* gene expression in TAMR EFM19 cells than in parental EFM19 cells (Fig. 3E and F). The tumor suppressor gene p53 triggers cell cycle arrest through stabilization and activation of CDKN1A, which encodes the CDK inhibitor p21[30]. Both p53 and p21 play pivotal roles in cancer cell dormancy[23,31,32]. Although long-term exposure to tamoxifen reduces the proliferation and migration of

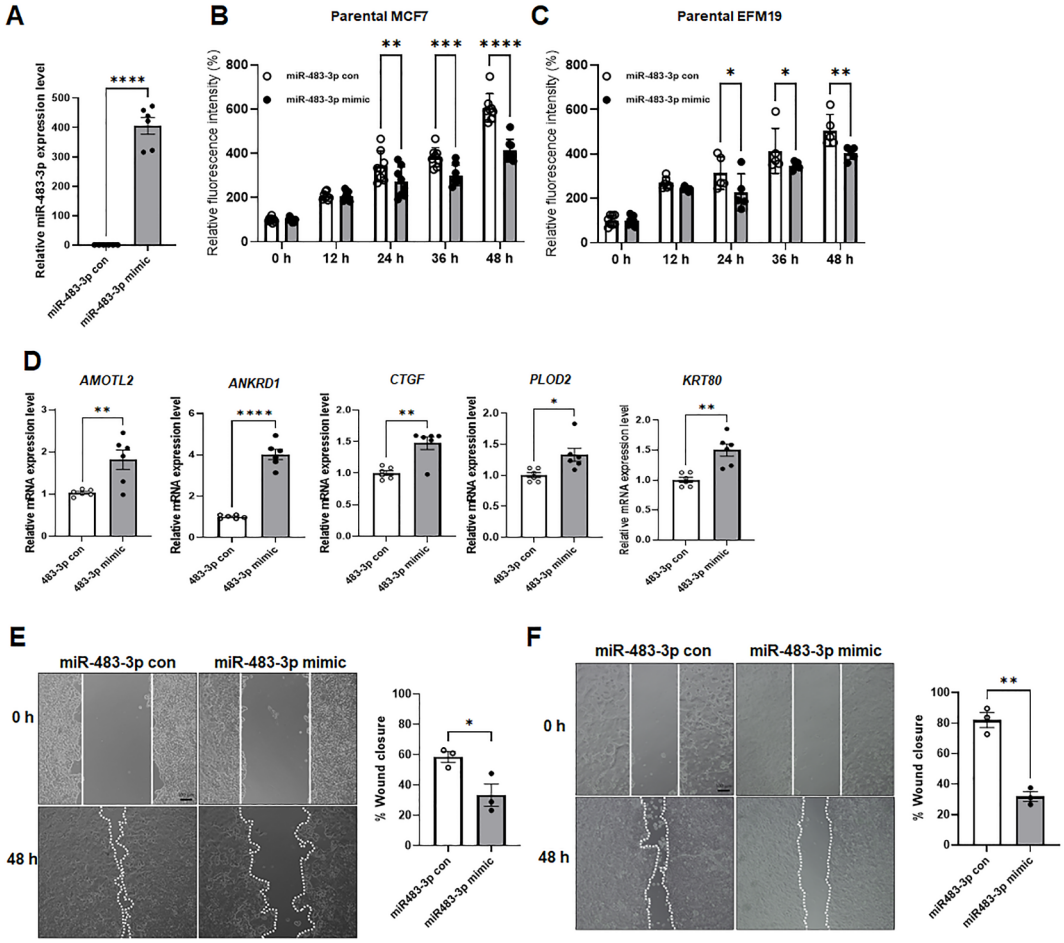

Fig. 4. miR483-3p mimics dormancy-like features of breast cancer cells. (**A**) The expression level of miR483-3p was evaluated using qRT-PCR in parental EFM19 cells after transfection with miRNA control or miR483-3p mimic (unpaired *t*-test, $^{****}p < 0.0001$, $n = 3$). (**B**) and (**C**) Parental EFM19 cells transfected with miRNA control or miR483-3p mimic were evaluated for their proliferation rate at 12 h up to 48 h. Cell viability was assessed using the alamarBlue assay (Two-way ANOVA, $^{*}p < 0.05$, $^{**}p < 0.01$, $^{***}p < 0.001$, and $^{****}p < 0.0001$). (**D**) Gene expression levels of *AMOTL2*, *ANRKD1*, *CTGF*, *PLOD2*, and *KRT80* in parental EFM19 cells transfected with miRNA control or miR483-3p mimic were evaluated using qRT-PCR ($n = 3$ independent experiments, unpaired *t*-test, $^{*}p < 0.05$, $^{**}p < 0.01$, $^{****}p < 0.0001$). Wound healing ability of parental MCF7 (**E**) and EFM19 (**F**) cells transfected with miRNA control or miR483-3p mimic. Photos were taken at 0 h and 48 h. The closed area indicated with a white line was quantified using ImageJ software. Scale bar = 100 µm. Graphs show the calculated wound closure percentage as mentioned in the Methods section (unpaired *t*-test, $^{*}p < 0.05$, $^{**}p < 0.01$).

breast cancer cells, it does not induce cell death. A recent study reported an inverse correlation between OGT and p21 expression, with reduced OGT levels increasing p21 protein levels, decreasing cell proliferation, and arresting the cell cycle without inducing cell death[33]. This implies that the observed elevation in p53 and p21 levels may have resulted from reduced OGT expression.

Previous studies have highlighted the potential of specific miRNAs as biomarkers for early breast cancer diagnosis even before detection through imaging[34–37]. Various miRNAs have been implicated in these studies, with associations reported between miRNA panels and signaling pathways, such as Rap1, MAPK, Wnt, and cGMP-PKG[38]. Another focus of miRNA research in breast cancer is metastasis, with miR-29a, miR-103/107, miR-155, miR-7, the miR-200 family, miR-205, miR-448, miR-181, and miR-661 associated with EMT, cell invasion, and proliferation[39,40]. The role of miR-483-3p is not yet well-defined; however, it has been reported to suppress the proliferation and progression of human triple negative breast cancer cells by targeting the oncogene HDAC8[41] or tumor showed tumor suppression in ER + PR + HER- luminal A subtype breast cancer through targeting the cyclin E1 gene[42].

However, the mechanisms by which persistent endocrine therapy induces miR-483-3p expression and how dormant breast cancer cells resume tumorigenesis remain unclear. Recent studies have suggested that epigenetic changes may induce dormancy and relapse in patients with ERP breast cancer[43]. Increased histone repressive markers (H3K9me2, H3K27me3, and H4K20me3) were observed in the late-relapse cohorts. Dormant epigenome instability and progressive loss of histone repressive markers may trigger cell proliferation, mimicking patient

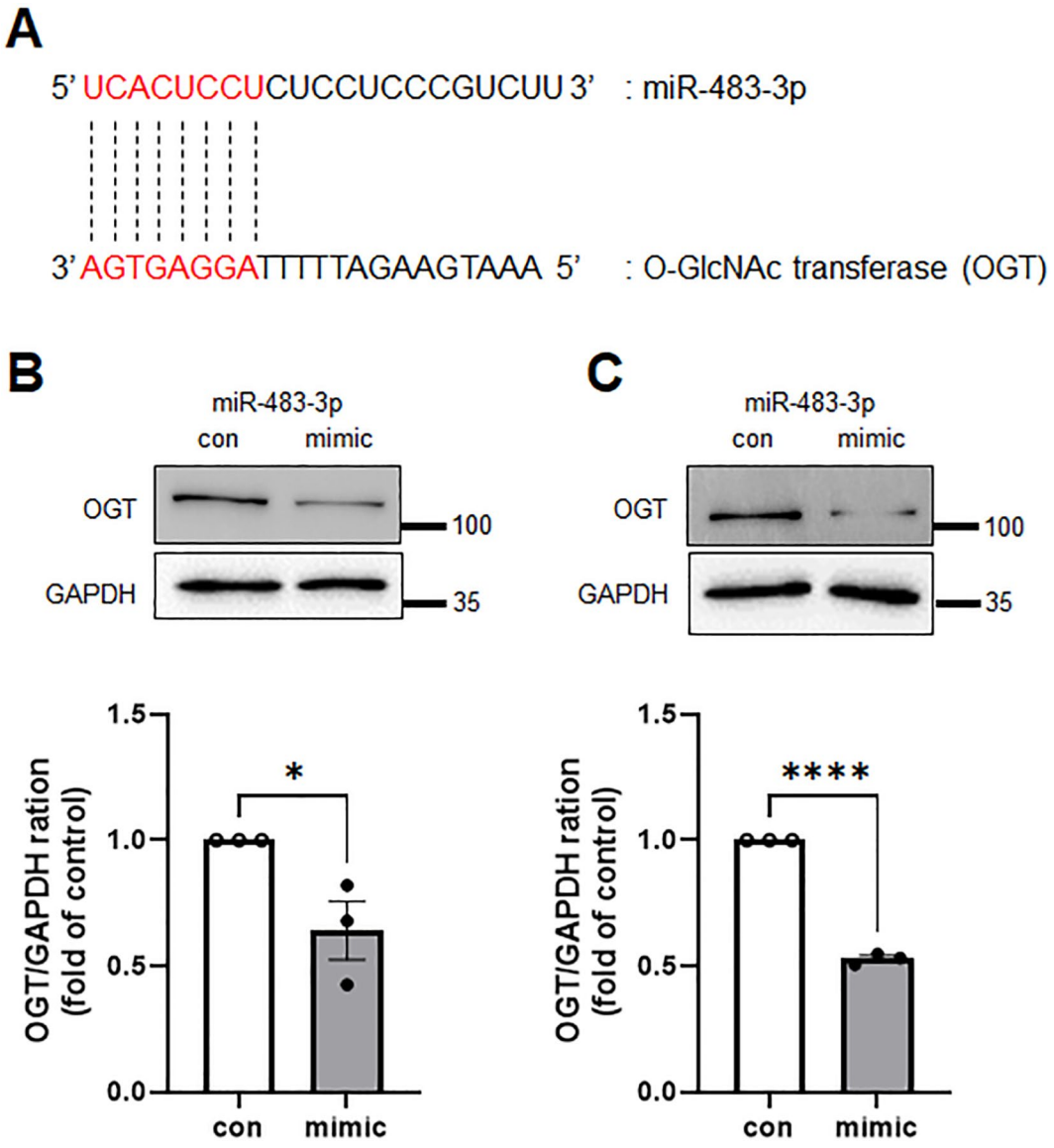

Fig. 5. miR483-3p interrupts the expression of OGT. (**A**) miR483-3p binding sites in the 3'UTR of OGT based on TargetScan prediction. Immunoblot analysis was conducted on parental MCF7 (**B**) and EFM19 (**C**) cells transfected with miRNA control or miR483-3p. Graph shows the quantification of the protein expression levels of OGT compared with GAPDH ($n = 3$, unpaired t-test, $^{*}p < 0.05$, $^{****}p < 0.0001$).

relapse. ER and co-regulator recruitment to chromatin are highly coordinated to ensure proper transcriptional and repressive activity at ER target sites, which may be disrupted by persistent ER inhibition[44,45]. Further studies are required to elucidate the involvement of epigenetic change and/or miRNA regulation.

In this study, we confirmed that miR483-3p is involved in dormancy in breast cancer during long-term endocrine therapy. Our study has certain limitations due to the small number of patient samples; however, it is significant in identifying miRNAs that may induce dormancy in breast cancer patients experiencing late recurrence. Future research should aim to secure a larger cohort of patient samples to further elucidate the mechanisms underlying the increased expression of miR483-3p during long-term hormone therapy and its regulation of OGT expression. These finding suggests the potential to diagnose breast cancer with delayed recurrence, thereby improving the efficiency of cancer treatment by selectively targeting recurrent breast cancer.

Conclusions

Overall, our findings suggest that miR-483-3p may serve as an indicator of delayed recurrence in patients undergoing long-term endocrine therapy, highlighting its potential as a biomarker for identifying patients at risk of delayed recurrence. This study is the first to identify miRNAs related to late recurrence of breast cancer and to elucidate their mechanisms, providing significant insights for treatment decisions and prognosis predictions in patients with luminal-type breast cancer.

Data availability

The datasets used and or analyzed during the current study available from the corresponding author on reasonable request.

Received: 7 August 2024; Accepted: 23 December 2024
Published online: 03 January 2025

References

1. Demicheli, R. et al. Recurrence and mortality according to estrogen receptor status for breast cancer patients undergoing conservative surgery. Ipsilateral breast tumour recurrence dynamics provides clues for tumour biology within the residual breast. *BMC Cancer*. **10**, 656 (2010).
2. Davies, C. et al. Long-term effects of continuing adjuvant tamoxifen to 10 years versus stopping at 5 years after diagnosis of oestrogen receptor-positive breast cancer: ATLAS, a randomised trial. *Lancet* **381**, 805–816 (2013).
3. Ribnikar, D., Sousa, B., Cufer, T. & Cardoso, F. Extended adjuvant endocrine therapy - A standard to all or some? *Breast* **32**, 112–118 (2017).
4. Park, Y. H. et al. Pan-asian adapted ESMO Clinical Practice guidelines for the management of patients with early breast cancer: A KSMO-ESMO initiative endorsed by CSCO, ISMPO, JSMO, MOS, SSO and TOS. *Ann. Oncol.* **31**, 451–469 (2020).
5. Burstein, H. J. et al. Adjuvant endocrine therapy for women with hormone receptor-positive breast cancer: American Society of Clinical Oncology Clinical Practice Guideline focused update. *J. Clin. Oncol.* **32**, 2255–2269 (2014).
6. Al-Mubarak, M. et al. Extended adjuvant tamoxifen for early breast cancer: A meta-analysis. *PLoS One*. **9**, e88238 (2014).
7. Calin, G. & Croce, C. M. MicroRNA signatures in human cancers. *Nat. Rev. Cancer*. **6**, 857–866 (2006).
8. He, L. et al. A microRNA component of the p53 tumour suppressor network. *Nature* **447**, 1130–1134 (2007).
9. Calin, G. & Croce, C. M. MicroRNAs and chromosomal abnormalities in cancer cells. *Oncogene* **25**, 6202–6210 (2006).
10. Chang, T. et al. Widespread microRNA repression by Myc contributes to tumorigenesis. *Nat. Genet.* **40**, 43–50 (2008).
11. O'Donnell, K., Wentzel, E. A., Zeller, K. I., Dang, C. V. & Mendell, J.T. c-Myc-regulated microRNAs modulate E2F1 expression. *Nature* **435**, 839–843 (2005).
12. Esteller, M. Non-coding RNAs in human disease. *Nat. Rev. Genet.* **12**, 861–874 (2011).
13. Calin, G., Croce, C.M. et al. A MicroRNA signature associated with prognosis and progression in chronic lymphocytic leukemia. *N Engl. J. Med.* **353**, 1793–1801 (2005).
14. Wang, J., Chen, J. & Sen, S. microRNA as biomarkers and diagnostics. *J. Cell. Physiol.* **231**, 25–30 (2016).
15. Valera, V. A., Parra-Medina, R., Walter, B. A., Pinto, P. & Merino, M. J. microRNA expression profiling in young prostate cancer patients. *J. Cancer*. **11**, 4106–4114 (2020).
16. Zhu, Y. et al. Tamoxifen-resistant breast cancer cells are resistant to DNA-damaging chemotherapy because of upregulated BARD1 and BRCA1. *Nat. Commun.* **9**, 1595 (2018).
17. Kim, H. et al. CTGF and Cyr61 are overexpressed in tamoxifen-resistant breast cancer and induce transcriptional repression of ERα. *J. Cell. Sci.* **134**, 1–18 (2021).
18. Li, X. et al. YAP inhibits ERα and ER + breast cancer growth by disrupting a TEAD-ERα signaling axis. *Nat. Commun.* **13**, 3075 (2022).
19. Ma, S. et al. Transcriptional repression of estrogen receptor alpha by YAP reveals the Hippo pathway as therapeutic target for ER + breast cancer. *Nat. Commun.* **13**, 1061 (2022).
20. Chen, H. et al. LTBP-2 confers pleiotropic suppression and promotes dormancy in a growth factor permissive microenvironment in nasopharyngeal carcinoma. *Cancer Lett.* **325**, 89–98 (2012).
21. Tivari, S., Lu, H., Dasgupta, T., De Lorenzo, M. S. & Wieder, R. Reawakening of dormant estrogen-dependent human breast cancer cells by bone marrow stroma secretory senescence. *Cell. Commun. Signal.* **16**, 48 (2018).
22. Shen, S., Vagner, S. & Robert, C. Persistent cancer cells: The deadly survivors. *Cell* **183**, 860–874 (2020).
23. Fares, J., Fares, M. Y., Khachfe, H. H., Salhab, H. A. & Fares, Y. Molecular principles of metastasis: A hallmark of cancer revisited. *Signal. Transduct. Target. Ther.* **5**, 28 (2020).
24. Akella, N. M. et al. O-GlcNAc transferase regulates cancer stem-like potential of breast cancer cells. **18**, 585–598 (2020).
25. Leturcq, M. et al. O-GlcNAc transferase associates with the MCM2–7 complex and its silencing destabilizes MCM–MCM interactions. *Cell. Mol. Life Sci.* **75**, 4321–4339 (2018).
26. Akella, N. M., Ciraku, L. & Reginato, M. J. Fueling the fire: Emerging role of the hexosamine biosynthetic pathway in cancer. *BMC Biol.* **17**, 52 (2019).
27. Ferrer, C. M., Sodi, V. L. & Reginato, M. J. O-GlcNAcylation in cancer biology: Linking metabolism and signaling. *J. Mol. Biol.* **428**, 3282–3294 (2016).
28. Zeidan, Q., Wang, Z., De Maio, A. & Hart, G. W. O-GlcNAc cycling enzymes associate with the translational machinery and modify core ribosomal proteins. *Mol. Biol. Cell.* **21**, 1922–1936 (2010).
29. Guo, H. et al. Acetylglucosamine (O-GlcNAc) expression levels epigenetically regulate colon cancer tumorigenesis by affecting the cancer stem cell compartment via modulating expression of transcriptional factor MYBL1. *J. Biol. Chem.* **292**, 4123–4137 (2017).
30. Chen, J. The cell-cycle arrest and apoptotic functions of p53 in tumor initiation and progression. *Cold Spring Harb Perspect. Med.* **6**, a026104 (2016).
31. Abbas, T. & Dutta, A. p21 in cancer: Intricate networks and multiple activities. *Nat. Rev. Cancer*. **9**, 400–414 (2009).
32. Karimian, A., Ahmadi, Y. & Yousefi, B. Multiple functions of p21 in cell cycle, apoptosis and transcriptional regulation after DNA damage. *DNA Repair. (Amst)*. **42**, 63–71 (2016).
33. de Queiroz, R. M., Moon, S. H. & Prives, C. O-GlcNAc transferase regulates p21 protein levels and cell proliferation through the FoxM1–Skp2 axis in a p53-independent manner. *J. Biol. Chem.* **289**, 102289 (2022).
34. Kahraman, M. et al. MicroRNA in diagnosis and therapy monitoring of early-stage triple-negative breast cancer. *Sci. Rep.* **8**, 11584 (2018).
35. Li, M. et al. A five-miRNA panel in plasma was identified for breast cancer diagnosis. *Cancer Med.* **8**, 7006–7017 (2019).
36. Zubair, M., Wang, S. & Ali, N. Advanced approaches to breast cancer classification and diagnosis. *Front. Pharmacol.* **202**(11), 632079.
37. Hannafon, B. N. et al. Plasma exosome microRNAs are indicative of breast cancer. *Breast Cancer Res.* **18**, 90 (2016).
38. Chen, X. et al. Breast invasive ductal carcinoma diagnosis with a three-miRNA panel in serum. *Biomark. Med.* **15**, 951–963 (2021).
39. Taylor, M. A., Sossey-Alaoui, K., Thompson, C. L., Danielpour, D. & Schiemann, W. P. TGF-β upregulates miR-181a expression to promote breast cancer metastasis. *J. Clin. Invest.* **123**, 150–163 (2013).
40. Wang, L. & Wang, J. MicroRNA-mediated breast cancer metastasis: From primary site to distant organs. *Oncogene* **31**, 2499–2511 (2012).
41. Menbari, M. N. et al. Mir-483-3p suppresses the proliferation and progression of human triple negative breast cancer cells by targeting the HDAC8 > oncogene. *J. Cell. Physiol.* **235**, 2631–2642 (2020).
42. Huang, X. & Lyu, J. Tumor suppressor function of mir-483-3p on breast cancer via targeting of the cyclin E1 gene. *Exp. Ther. Med.* **16**, 2615–2620 (2018).

43. Rosano, D. et al. Long-term multimodal recording reveals epigenetic adaptation routes in dormant breast cancer cells. *Cancer Discov.* **14**, 866–889 (2024).
44. Garcia-Martinez, L., Zhang, Y., Nakata, Y., Chan, H. L. & Morey, L. Epigenetic mechanisms in breast cancer therapy and resistance. *Nat. Commun.* **12**, 1786 (2021).
45. Johnson, A. B. & O'Malley, B. W. Steroid receptor coactivators 1, 2, and 3: Critical regulators of nuclear receptor activity and steroid receptor modulator (SRM)-based cancer therapy. *Mol. Cell. Endocrinol.* **348**, 430–439 (2012).

Author contributions
All authors contributed to the conception and design of this study. Material preparation, data collection, and analyses were performed by OHK, TJJ, HK, ESC, SAH, MKK, and HJL. OHK, TJJ, MKK and HJL wrote the first draft of the manuscript. MKK and HJL made critical revisions. All authors have approved the version of the manuscript for publication.Figure 1 made by SAH and MKK. Figure 2 made by OHK, TJJ, HK, ESC and HJL. Figure 3 made by OHK, TJJ and HJL. Figure 4 made by OHK and HJL. Figure 5 made by OHK and HJL.

Funding
This work was financially supported by a National Research Foundation of Korea (NRF) grant funded by the Korean government (Grant nos. 2023R1A2C2006894, 2020R1A2C2011617 and 2020R1G1A1102425) and by a grant of the Korean Cancer Survivors Healthcare R&D Project through the National Cancer Center, funded by the Ministry of Health & Welfare, Republic of Korea (RS-2023-CC139876).

Declarations

Competing interests
The authors declare no competing interests.

Ethics approval and consent to participate
For human samples, approval was obtained from the Institutional Review Board of Chung-Ang University Hospital (IRB number 2301-019-539). A waiver of informed consent was granted by the Institutional Review Board of Chung-Ang University Hospital.

Additional information
Supplementary Information The online version contains supplementary material available at https://doi.org/10.1038/s41598-024-84437-6.

Correspondence and requests for materials should be addressed to M.K.K. or H.J.L.